Aerodynamic Analysis of A Ski Jumper: A CFD Approach

Richie Latchman and Akash Pooransingh
Department of Electrical and Computer Engineering
The University of the West Indies, St. Augustine Campus
Email: richielatchman@hotmail.com, akash.pooransingh@sta.uwi.edu

Abstract:
Wind tunnel experiments on ski jumpers have shown that changes in posture result in distinct changes to the lift and drag areas. The disadvantages of performing these tests have led to the proposition of CFD as a possible alternative. This study involved developing a computational model of the ski jumper, performing simulations using the k-ε and SST turbulence models and comparing the simulated results with experimental results. While some characteristics of the measured data were observed in the simulated data, it was concluded that further geometric complexities need to be added to the computational model and more refined meshes are required. This study reveals that the SST turbulence model is quite suited to this application and requires further investigation.

Keywords: CFD, Solidworks, k-ε turbulence model, SST turbulence

1. Introduction

At the 2006 Winter Olympics, the jump length difference between first and second place was only 5cm. This illustrates why ski jumpers are constantly tinkering with their posture in order to gain even the smallest of advantages. Experiments such as those shown in Figure 1, conducted with ski jumpers in large-scale wind tunnels showed that changes in position can lead to marked changes in the lift and drag forces. These comprehensive experiments in large-scale wind tunnels involving very detailed modifications, however, involve excessive measurement time and costs, and require that world-class athletes be available for unreasonably long periods (Meile et al, 2006).

Commercial Computational Fluid Dynamics (CFD) simulation tools are now being utilized for sporting applications as an alternative to wind tunnel measurements to predict flow field and evaluate aerodynamic forces. The Magnus Effect of a soccer ball was illustrated by Fontes (2014) and conventional swing of a cricket ball

Figure 1. Wind tunnel measurements with A. Goldberger (Muller, 2008)

was modelled by Latchman and Pooransingh (2015). Meile et. al (2006) investigated the possibility of using CFD as an alternative for optimizing lift and drag of ski jumpers. The comparison of their simulation and experimental results showed poor agreement. They explained that the difference in results could be as a result of too coarse a mesh or the unsuitability of k-ε turbulence model used. They recommended that further work using more advanced turbulence models and refined meshes was required. They also noted that the human body model used consisted of geometrically simple bodies, prismatic in nature. The geometrical difference between the model used and the actual human body may also account for discrepancies in the results.

This study uses the CFD module of COMSOL Multiphysics® in the aerodynamic analysis of a ski jumper. Building on the work and recommendations of Meile et. al (2006), the k-ε and SST (Shear Stress Transport) turbulence models will be used. Geometric complexities will be added to their initial model and the meshing will be refined as much as possible within the limitations of the system used to conduct the simulations.

2. Theory

Professional ski jumpers currently use the V-technique in which during the flight phase the skis are not held parallel to each other. This technique allows the jumper to lean forward in a more distinct manner which produces lift and drag forces that improves the aerodynamics of the jumper when compared to the old parallel technique. As a result, at a given in-run velocity, using the V-technique will produce a greater jump length.

Figure 2 shows the angle nomenclature that is used when measuring the flight position of the ski jumper when analysing flight styles. α is the angle of attack of the skis, β is the body to ski angle, γ is the hip angle, δ is the head angle, φ is the arm angle and the angle of the skis to each other is V.

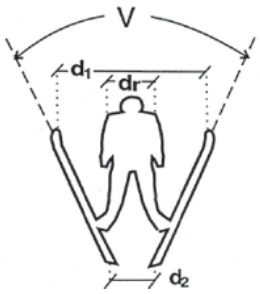

(a) V-style parameters (Muller, 2008)

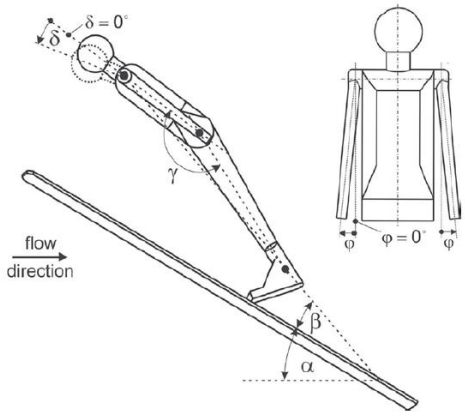

(b) Simplified model of a ski jumper in typical posture and flight position. (Meile et al, 2006)

Figure 2. Angle nomenclature of the V-style

The ski jumper varies the angle of attack and the positioning of body parts and skis during flight in order to maximize the jump length. High lift forces are desired throughout the flight while the disadvantage of high drag has a greater effect during the first flight phase. As such ski jumpers and their coaches focus their efforts on improving the flight styles. This led to the idea of performing basic studies on the aerodynamics of ski jumping using CFD to reduce time, costs and athlete disposability. (Meile et al, 2006)

The lift and drag forces are given by the following expressions:

$$F_l = \frac{1}{2}\rho L w^2$$

$$F_d = \frac{1}{2}\rho D w^2$$

where L is the lift area, D is the drag area, ρ is the air density and w is the wind velocity. (Muller, 2008)

3. Method and Use of COMSOL Multiphysics® Software

3.1 Pre-process of CFD Analysis

3.1.1 Creation of the computational model of a ski jumper and the computational domain.

The aerodynamics of bluff bodies continues to be a challenging task for turbulence simulation tools. Simplifications to the geometry of the computation model of a ski jumper are therefore required. Reisenberger et al. (2004) proposed the idea of representing the human body by a combination of geometrically simple bodies for CFD analysis. Based on this, Meile et. al (2006) conducted CFD investigations on a ski jumper model that consisted of geometrically simple bodies that were prismatic in shape as shown in Figure 2b.

This study introduces additional geometric complexities to the computational model of the ski jumper used for CFD analysis. Using the dimensions of an average built human body; the computational model shown in Figure 3 was developed in SOLIDWORKS®. This model was imported into the model builder of COMSOL Multiphysics® using the LiveLink™ for SOLIDWORKS®. The ski jumper was modeled as a homogeneous nylon material since it is common that ski jumpers wear suits that are made of primarily of this material. It must also be noted that the composite nature of the human

body has no effect on the development of the fluid flow profile around the ski jumper.

Figure 3. Computational model of the ski jumper developed in SOLIDWORKS®.

In order to evaluate the possibilities and/or limits of CFD, a variety of selected postures of the computational model of the ski jumper will be simulated numerically and compared with measurements made by previous researchers. As such, the jumper's computational model was developed in SOLIDWORKS® to allow for the posture angles to be easily adjusted. This was achieved by using component parts of the human body model and creating an assembly with suitable mates.

The computational domain which is the geometry for the flow region is a significant feature of any CFD model. The length of the computational domain must allow for the flow dynamics to be sufficiently developed while the width and height must be prescribed to negate the boundary effects so that it does not influence the flow. These dimensions must, however, be kept to a minimum so that CFD calculations are still manageable and does not significantly increase the simulation time. The computational domain used is a rectangular parallelepiped having dimensions of 300 cm x 325 cm x 600 cm in the x, y and z directions respectively. The computational model of the ski jumper was placed at a suitable distance from the inlet boundary as shown in Figure 4 to capture the downstream effects effectively. (Jiyuan, Yeoh and Liu 2008, 35).

3.1.2 Selection of Fluid Properties and Physics

In the absence of external forces, incompressible Newtonian fluid flow is assumed. The fluid flow around the ski jumper is modeled by the Reynolds-Averaged Navier-Stokes (RANS) equations. The k-ε and SST turbulence models within COMSOL Multiphysics® will be used to simulate the flow. The standard k-ε turbulence model is the simplest model out of the variety of available turbulence models but is the most robust. Thus it must be used as the starting point in the evaluation of CFD for aerodynamic analysis of the ski jumper. The k-ε turbulence model, however, uses a wall function formulation which reduces its accuracy. The SST model does not use wall functions and is more accurate when solving for the flow near the wall. (Frei, 2013)

3.1.3 Mesh Generation

Tetrahedral cells were used for the mesh generation as shown in Figure 4. A predefined finer mesh was used for the computational model of the ski jumper. It consisted of approximately 45,500 domain elements with a maximum element size of 37.5 cm while the minimum element size was 2.73 cm. The elements of this mesh were calibrated for general physics. For the computational domain, a predefined coarser mesh was used consisting of approximately 329,500 domain elements with a maximum element size of 52.9 cm while the minimum element size was 16.3 cm. For simulations using the k-ε model, the mesh of the computational domain was refined to a predefined coarse mesh contained approximately 470,000 domain elements with a maximum element size of 40.7 cm while the minimum element size was 12.2 cm. The mesh elements of the computational domain were calibrated for fluid dynamics. The number of degrees of freedom solved when using the coarser and coarse meshes were approximately 350,000 and 400, 000 respectively.

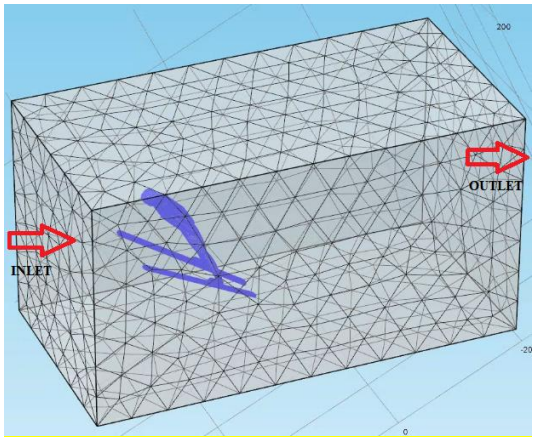

Figure 4. Computational model of the ski jumper in the computational domain showing the inlet and outlet boundaries

3.1.4 Specification of Boundary Conditions

Wind tunnel testing is based on the principle that the flow profile developed around an object moving at a specified velocity through still air is the same as that of air of the specified velocity moving over the stationary object. This principle will be applied in developing the model to simulate the flow around the ski jumper. (NASA, 2014)

Figure 4 shows the inlet and outlet boundaries for the computational domain. The remaining four surfaces of the computational domain are open boundaries. The following boundary conditions were specified:

- The inlet condition was specified by a normal inflow velocity of 30 m/s.
- The outlet condition was specified by a pressure of 0 Pa.
- A symmetry boundary condition was specified for the open boundaries.

3.3 Post process of the CFD Analysis

The CFD module of COMSOL Multiphysics generates three types of plots for the results of a simulation.

1. Velocity magnitude – illustrates the flow velocity around the computational model.
2. Surface contour of pressure – illustrates the pressure distribution.
3. Wall resolution – the wall lift-off plot can be used to check the accuracy of the solution.

3.3.1 Determination of the drag and lift force

According to Lyu (2015), lift and drag forces are comprised of a pressure component and viscous component. The pressure component is due to the pressure difference across the surface while the viscous component is due to friction that acts opposite to the flow direction.

Within COMSOL Multiphysics®, the simplest way to compute drag and lift forces is to integrate the total stress, which comprises of the pressure and viscous forces, in the respective directions. The integration is done by defining a surface integration operator under the Derived Values node.

Since the k-ε turbulence model utilizes a wall function, using the friction velocity computes the viscous force more accurately. The local shear stress at the wall is calculated using

$$u_\tau = \sqrt{\frac{\tau_w}{\rho}}$$

Therefore, the local shear stress in the y-direction is:

$$\tau_{w_y} = \rho u_\tau^2 \frac{u_y^T}{u^T}$$

where u^T is the tangential velocity at the wall. u^T can be written as $u_\tau * u^+$, where u^+ is the tangential dimensionless velocity.

The pressure force in the y-direction is determined by multiplying pressure by the y-component of the normal vector on the surface. This is done to project the scalar variable of pressure in the direction of y.

Table 1. Summary of the expressions that will be integrated in the y-direction to compute the respective forces in that direction.

	Without Wall Function	*With Wall Function*
Pressure Force	spf.nymesh*p	spf.nymesh*p
Viscous Force	spf.K_stressy	spf.rho*spf.u_tau* spf.u_tangy/spf.uPlus
Total Force	spf.T_stressy	spf.nymesh*p + spf.rho*spf.u_tau*spf .u_tangy/spf.uPlus

The corresponding expressions from Table 1, for the z-direction will be used to compute those forces. In determining the lift and drag forces expressions, a correction will be made for the angle of attack by resolving the total forces in the y and z directions in the directions of lift and drag

4. Governing Equations

The Reynolds-Averaged Navier-Stokes (RANS) Equations for an incompressible and Newtonian fluid are given by

$$\rho\frac{\partial \boldsymbol{u}}{\partial t} + \rho(\boldsymbol{u}\cdot\nabla)\boldsymbol{u} = \nabla\cdot[-p\boldsymbol{I} + \mu(\nabla\boldsymbol{u} + (\nabla\boldsymbol{u})^T)] + \boldsymbol{F}$$
$$\rho\nabla\cdot\boldsymbol{u} = 0$$

where

- ρ is the density
- **u** is the velocity vector
- p is pressure
- **F** is the volume force vector

The *k*-ε turbulence model introduces two additional transport equations and two dependent variables: the turbulent kinetic energy, k, and the dissipation rate of turbulence energy, ε.

The SST turbulence model combines the performance of the *k*-ω model near in the near-wall region with the robustness of the *k*-ε by interpolating between the two. The model equations are formulated in terms of *k* and ω, where ω is the specific dissipation rate.

5. Results

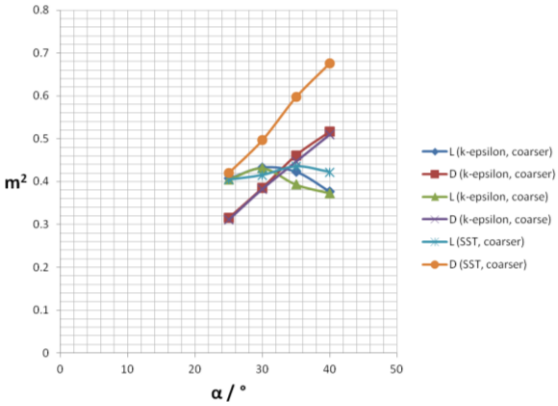

Figure 5. Variation of the L and D with α when β = 15°, ϒ = 160°, V = 35° and δ = 0° (See Appendix)

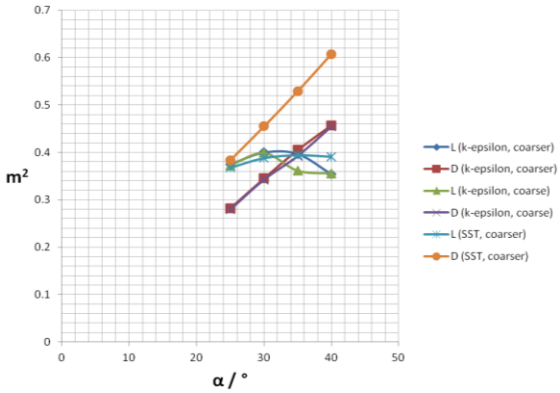

Figure 6. Variation of the L and D with α when β = 20°, ϒ = 160°, V = 35° and δ = 0° (See Appendix)

Figures 5 and 6 show the variation of L and D with α for β equal to 15° and 20°. The graphs of all models exhibit similar characteristics to measurements made on Andreas Goldberger, World Cup winner 1994/95. The measurements made by Muller (2008), show that as α increases the value of D increases while L increases to a maximum value and then starts decreasing. Muller also observed that for α = 30°, γ = 160° and V = 35°, the value of L and D were almost the same for β = 15°. Both these observations can be made from Figures 5 and 6.

While the value of L in all the models are approximately the same, the value of D in the SST model is significantly different to that of the k-ε model. The values of L and D measured by Muller are not the same as those in Figures 5 and 6. The data, however, suggests that the SST model gives a more accurate result. Examination of the flow velocity profiles of the two models (Figures 7 and 8) show a significance in the wake developed.

Though the mesh of the computational domain of the k-ε model was refined, the change in values were insignificant. The wall lift-off plot (Figure 9) ranges from 54 to 1295 which inidcates that the result for this model is inaccurate because the mesh at the wall of the computational model is not fine enough. A value of 11.06 is desired and Frei (2013) recommends that a finer boundary layer mesh be used at the walls. Figure 10 illustrates the pressure distribution over the computational model of the ski jumper.

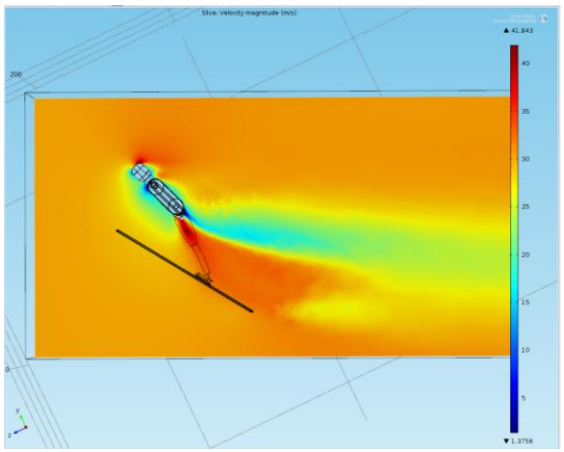

Figure 7. Velocity magnitude plot for the k-ε turbulence model using a coarser mesh for the computational model

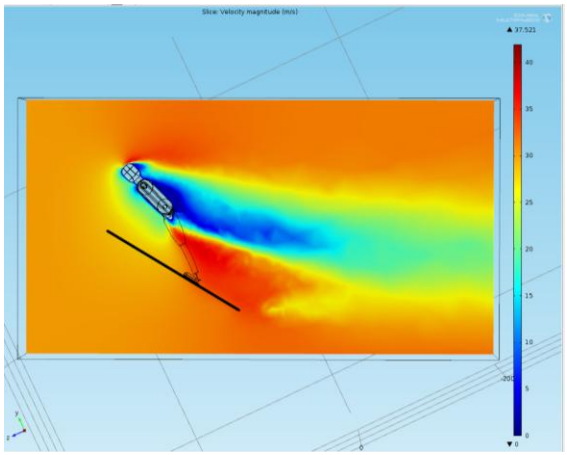

Figure 8. Velocity magnitude plot for the SST turbulence model using a coarser mesh for the computational model

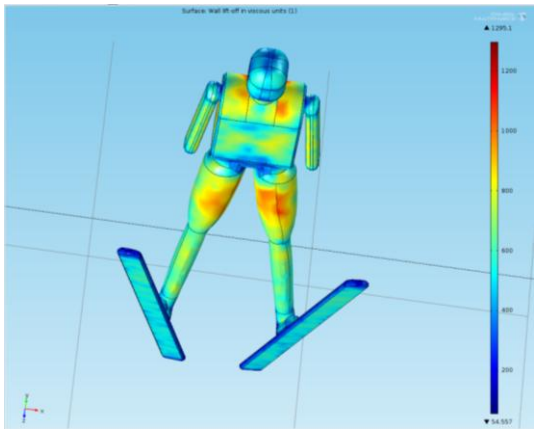

Figure 9. Wall lift-off plot of the k-ε model using the coarse mesh for the computational domain.

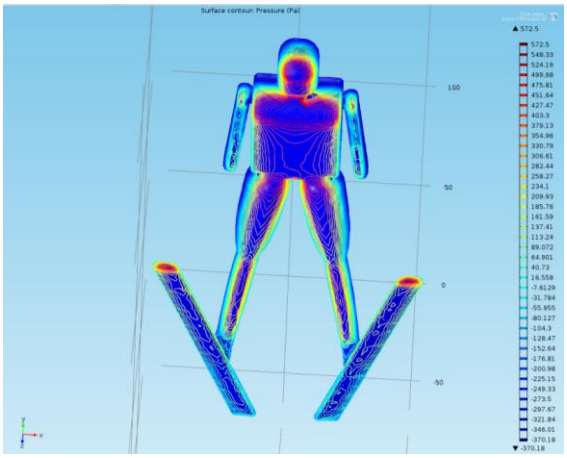

Figure 10. Surface contour pressure plot for the SST turbulence model using a coarser mesh for the computational model

6. Conclusion

From this study, the following similarities between the measured and simulated results were observed

- Drag area, D increased as the angle of attack, α increased when all other angles were held constant
- Lift area, L increased to a maximum and then decreased as the angle of attack, α increased when all other angles were held constant
- L and D had similar values when α = 30°, γ = 160°, V = 35°, β = 15°.

The difference in the measured and simulated results may be reduced by refining the mesh size used particularly around the wall of the computational model. The model can also be improved by adding new geometric complexities. The results of this study seem to indicate that the SST turbulence model is more suited to this application than the k-ε turbulence model and as such more detailed investigations should be carried out using this model.

7. References

1. B, Schmölzer and W Müller. The importance of being light: aerodynamic forces and weight in skijumping. Journal of biomechanics, 35(8), 1059-1069. (2002)

2. Ed, Fontes. The Magnus Effect and the World Cup Match Ball. COMSOL Blog. (2014).

3. National Aeronautics and Space Administration (NASA). “Wind Tunnel Testing” (2014) Accessed March 20, 2015. http://www.grc.nasa.gov/WWW/k-12/airplane/tuntest.html

4. Richie Latchman and Akash Pooransingh. Modeling Conventional Swing of a Cricket Ball Using COMSOL Multiphysics. COMSOL Conference, Boston. (2015).

5. Tu, Jiyuan, Guan Heng Yeoh and Chaoqun Liu. Computational Fluid Dynamics: A Practical Approach. Oxford: Elsevier. (2008)

6. W, Meile et al. Aerodynamics of ski jumping: experiments and CFD simulations. Experiments in fluids, 41(6), 949-964. (2006).

7. Walter, Frei. Which Turbulence Model Should I choose for My CFD Application? COMSOL Blog (2013)

8. Wolfram, Müller. Performance factors in ski jumping. Sport Aerodynamics: CISM Courses and Lectures, Vol 506, 139-160. (2008).

9. Wolfram, Müller. Computer simulation of ski jumping based on wind tunnel data. Sport Aerodynamics: CISM Courses and Lectures, Vol 506, 161-182. (2008).

8. Appendix

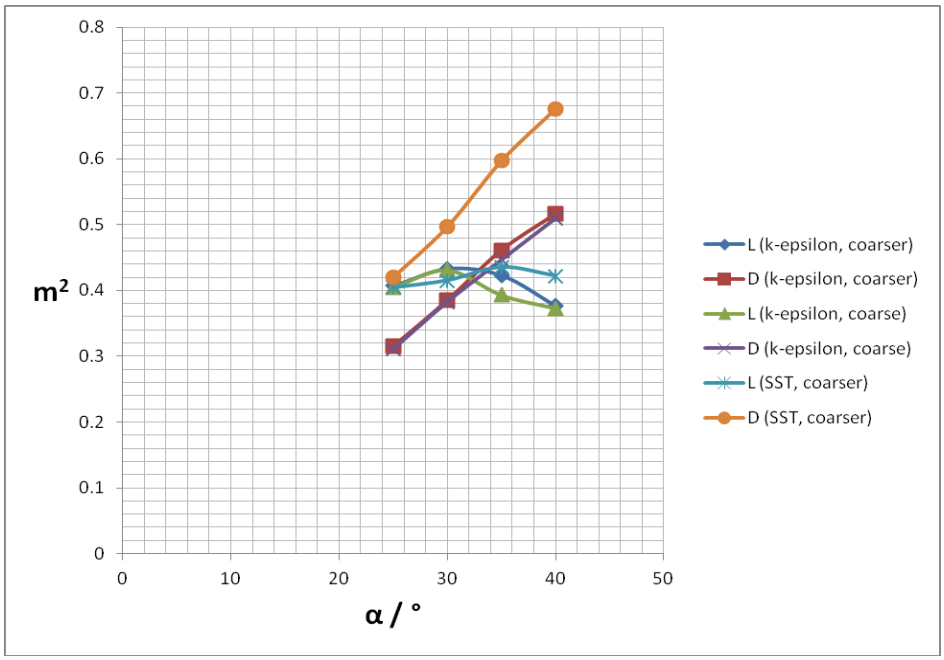

Figure 5. Variation of the L and D with α when β = 15°, ϒ = 160°, V = 35° and δ = 0°

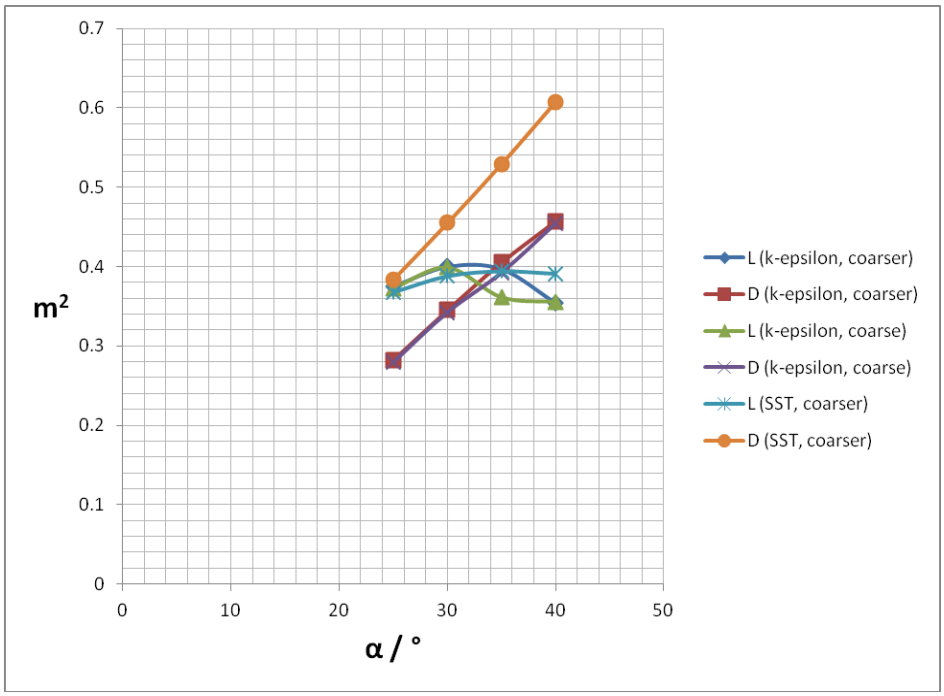

Figure 6. Variation of the L and D with α when β = 20°, ϒ = 160°, V = 35° and δ = 0°